Bioinspired Navigation Based on Distributed Sensing in the Leech using Dynamic Neural Fields

By
Sebastian Nichols

Senior Honors Thesis
The Department of Biology
University of North Carolina at Chapel Hill

May 5, 2021

Approved:

Brian Taylor, Thesis Advisor

Ty Hedrick, Reader

Paul Maddox, Reader

Abstract

Leeches use various sensory stimuli to navigate around their environment and perform survival behaviors. Water wave disturbances serve as an important source of environmental information for aquatic animals as they can be the distinguishing factor between a predator or prey. Previous studies show that certain leech species prefer specific frequencies of water waves, suggesting that the leech's sensory receptors have been evolutionarily calibrated to respond to wave frequencies in the safest way. While these animal studies provide important discoveries about the relationship between sensory information and animal behavior, the internal neural mechanisms driving the leech's decision-making are still unknown. In this study, we present a model that mimics the navigational behavior of the leech using dynamic neural fields and an agent-based simulation. The modeled leech (agent) was placed in virtual environments containing simulated stimuli based on the actual stimuli a leech detects in their natural environment. Sensors placed around the agent detected the stimulus and sent the sensory information to a neural field, which was responsible for calculating navigational behaviors. Data produced by the model matched real-world observed behaviors found in previous leech studies. The development and validation of this model offer a fast and low-cost way to study leech behavior, compliment animal experiments, and provide insights into the mechanics behind distributed sensing in animals. Additionally, the findings may provide insights into novel data-processing methods and architectures for man-made sensory systems that rely on multiple sensors.

1. Introduction

Distributed sensing refers to the spatial distribution of many sensors on an organism, allowing it to detect stimuli from single or multiple sensory modalities. Every animal with a nervous system uses an array of sensors (i.e., distributed sensing) to convert sensory stimuli to direct different behaviors (Fig. 1). For example, humans have low-threshold mechanoreceptors (LTMRs) dispersed across the epidermis that encode mechanical information, allowing us to determine where on our body a mechanical stimulus is located (Zimmerman et al., 2015). To successfully forage and survive, animals must be able to process

distributed sensory information to direct action under a multitude of environmental conditions. In addition, distributed sensing and nervous-system-like computing offers several potential benefits for engineered systems, including 1) robustness where many sensors must fail before the entire system fails, 2) the use of less complex and/or resource-intensive sensors to obtain actionable information about the world (Hochner, 2012), 3) the development of systems with lower size, weight, cost, and power requirements, 4), and improved adaptive navigation behavior (Mcdonnell et al., 2014).

Fig. 1 Example of visual sensilla on the head of a leech, showcasing one set of their distributed sensors (Govedich and Bain, 2005).

Leeches are a unique model organisms for studying neurobiology and distributed sensing due to their arrangement of over 294 distributed visual and mechanoreceptors. Scientists have studied the Medicinal leech's nervous system to understand the relationship between sensory stimulation, individual neuron behavior (i.e., spike rate frequency) and specific motor function (Lockery and Kristan, 1990; Kristan et al., 2005; Wagenaar, 2015; Moshtagh et al., 2013). However, the internal mechanisms by which a leech converts sensory information to motor behaviors are still unknown.

Previous experiments have studied sensing in the Medicinal leech, *Hirudo verbana* (Harley et al., 2011; Harley and Wagenaar, 2014). In these studies, leeches were exposed to different frequencies of

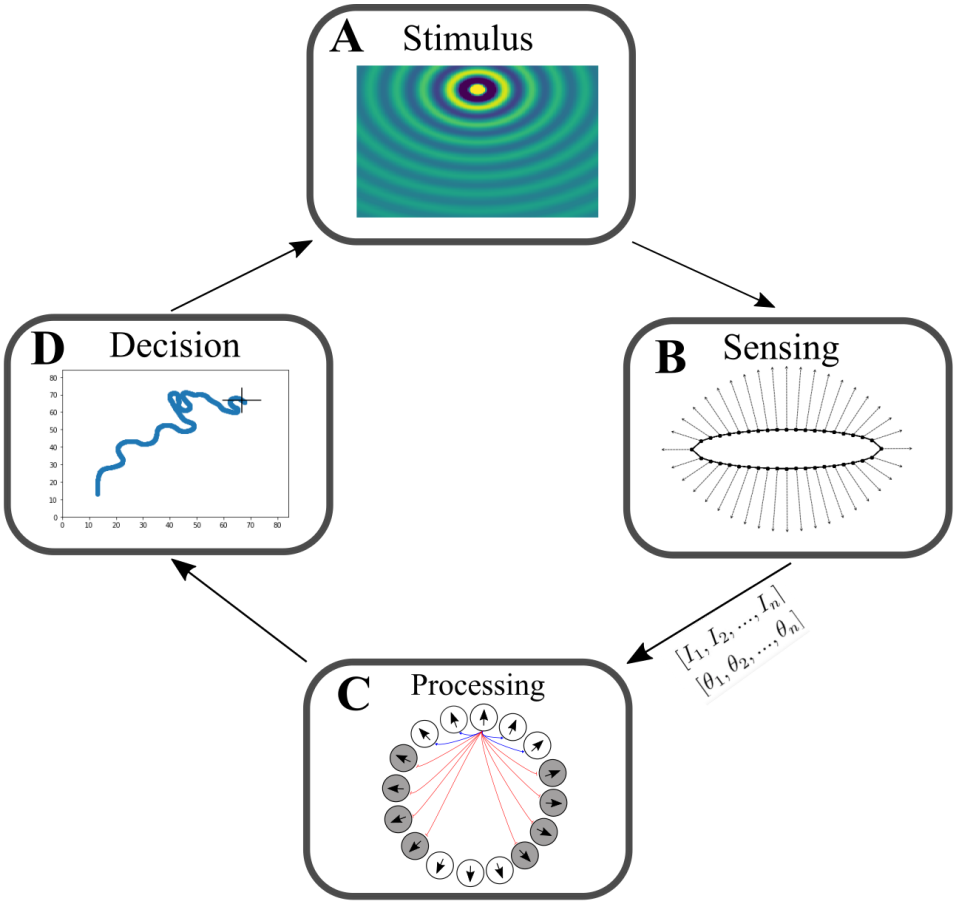

Fig 2. General flowchart displaying the core components of the model and how they interact with each other. Note that the simulation is a closed loop indicating that as the agent moves around in the simulated environment, the sensors are continuously updated to detect new water wave features. These sensors are arranged in a distributed manner, spanning around the perimeter of the agent (**B**). The sensors detect and gather information from the environment (**A**) which is sent to the neural field for neural processing (**C**). The neural field computes an angle that the agent uses to orient itself and navigate towards the target location (**D**).

water waves, which provided a variety of intensities of mechanical and visual stimuli in a laboratory-controlled environment. The physical motion of the water provides the mechanical stimulus (Fig. 2A), while the visual stimulus is generated by surface water waves creating a series of lenses that focus light at different spatial points (i.e., caustics). By measuring the percentage of leeches that successfully navigated to a target location (i.e., find rate), it was found that certain wave frequencies

produced maximal find rates for both unimodal and multimodal stimuli. This led to experiments that measured the spike rate of leech neurons (specifically, so-called S-cells which process multimodal sensory information) when stimulated by specific sensory frequencies and intensities both visually and mechanically (Lehmkuhl et al., 2018). The frequencies that generated the largest spike rates correlated with the frequencies that resulted in higher find rates, suggesting that the spike rates can be used as a behavioral predictor.

Various computational models have been implemented to simulate the neural response of neurons in animals (Jensen, 2010; Taylor, 2016; Taylor, 2017; Hunt et al., 2017; Zhang, 1996; Coombes et al, 2014; Kasabov, 2019). The previous iteration of this study used elliptical representations of spike rate distributions to mimic the leech's nervous system (Jenson, 2010; Nichols et at., 2020). The present study aims to build upon this simplified model and use dynamic neural fields for neural processing. Neural fields have been proven mathematically to recreate brain wave patterns and provide a framework to model the neural behavior of populations of distributed neurons (Amari, 1977 ; Coombes, 2014). One specific framework focuses on the neural excitation and inhibition between neural nodes within the network, known as a winner-take-all (WTA) network (Wilson, 1999). WTA networks can perform complex path integration computations such as vector summation, a calculation that involves adding together a sequence of perceived directions to find the quickest path back to a goal location (i.e., a rat taking a direct path back to its nest after randomly exploring its environment in search of food).

The experiments presented in this study display both the validation (section 3.1) and potential simulation experiments (section 3.2) that can be performed with the model. This study proposes a model that can sense (Fig. 2B), plan, and act based on the navigational behavior of a leech, using a WTA neural field model to generate biologically relevant neural activity (Fig. 2C). A behavioral algorithm transformed the neural responses into behavioral actions. A computer simulated agent then used these actions to navigate towards the center of a given mechanical stimulus (Fig. 2D). We analyzed the trajectories of the agent to verify that the model exhibits similar behavior to that of a leech. From a biological standpoint, our model can serve as a complementary testing tool alongside real-world leech experiments to help

discover the underlying mechanisms and principles of distributed sensing, sensor placement, and sensory detection. From an engineering standpoint, our model can be used in the development of man-made sensing, processing, and information systems and tools that are more precise, autonomous, and efficient.

2. Methods

The following section outlines the mathematical equations and relationships used to compute and simulate the mechanical stimulus, sensor detection, neural field processing, and motion control.

2.1 Simulated Water Waves

In order to mimic the behavior of the leech, we must first mimic the environmental conditions leeches face in their natural habitat. For this study we chose to focus on mechanosensory detection as a place to start, with hopes to incorporate visual sensing in the future. The simulated water waves were modeled as 2D surface waves with physical properties satisfying the dispersion relation, a relationship that defines how wavelength depends on wave frequency. The surface elevation of these waves can be modeled with the following equations,

$$n(x, y, t) = asin(\theta(x, y, t)) \quad \text{(Eq. 1a)}$$

$$\theta = 2\pi(\frac{x}{\lambda} - \frac{t}{T}) \quad \text{(Eq. 1b)}$$

$$k = \frac{2\pi}{\lambda}, \omega = \frac{2\pi}{T} \quad \text{(Eq. 1c)}$$

where n is the wave's elevation at time t and position (x, y) and a is the amplitude of the wave. Eq. 1b is the phase function of the wave, which describes the speed and frequency of wave propagation and depends on the time period (T) and wavelength (λ). A visual representation of this point source water wave is shown in the top panel of Fig. 2A, and Fig. 5. In this image, wavelength refers to the distance between two green peaks and a oscillates between 4 cm and -4 cm, depending on the distance from the target location (wave elevation dampens linearly as it travels further from the origin). Eq. 1c shows the relationships between the wavenumber (k) and wavelength, and the angular frequency (ω) and T. ω and k must satisfy the dispersion relation,

$$\omega^2 = gktanh(kh) \quad \text{(Eq. 1d)}$$

$$\lambda = \frac{g}{2\pi} tanh(2\pi \frac{h}{\lambda}) \quad \text{(Eq. 1e)}$$

where $tanh$ is the hyperbolic tangent. We chose to model water wave motion as being dependent on gravity and water depth (gravity waves) in order to generate baseline behavioral data in response to the simplest form of a mechanosensory stimulus. In future studies we would like to experiment with other water wave regimes such as capillary waves (water waves with motion governed by surface tension). The dispersion equation in Eq. 1d shows the spatial relationship of water movement based on the earth's gravitational constant (g) and water depth (h).

One of the goals of this study was to compare the model's navigational success as a function of wave frequency and wavelength to determine whether leeches detect wave frequency or wavelength. Since there is already data on leech navigation as a function of wave frequency, the wave frequencies were used as inputs into the dispersion relation to find wavelength (Harley et al., 2011). The fsolve function from python's scipy package solves Eq. 1e for wavelength at specific water depths and wave frequency inputs. k and the wave's direction were used as inputs into the sensor detection equation, as described in the next section.

2.2 Sensor Detection

Studies show that leeches use mechanosensory cells lined with cilia to detect shear, compression or tension forces, but it is still unknown exactly how cilia detect these mechanical forces (Bezares-Calderón et al., 2020). Since this study focuses on the neural processing of sensory information, a simplified model was used to simulate mechanosensation in the leech, as this method can be improved later with the neural processing remaining the same. This strategy assumes that because wave vectors carry information on the intensity of water motion, the magnitude of this wave vector (i.e., wavenumber k) can act as a proxy for mechanical force. Therefore, each sensor along the body of the simulated leech (agent) detects k and wave vector direction.

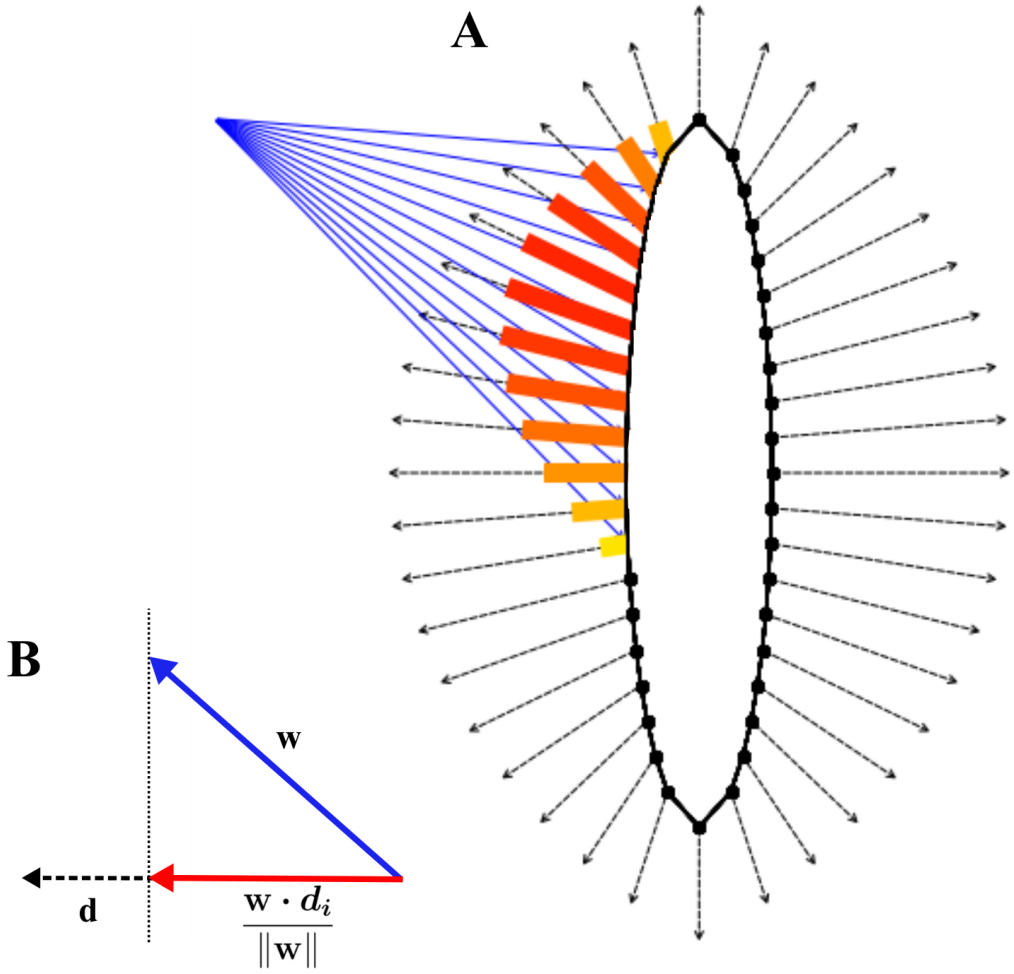

Fig 3. The mechanosensory detection method is displayed visually through an illustrated agent with its distributed sensors (black lines) and sample mechanosenory inputs shown as wave vectors (blue lines). The wave vectors carry information about the direction and magnitude of the oncoming water wave, which the agent can sense and process to orient itself towards the target location. The sensors detect the wave vector's normal component via vector projection (**B**). The magnitude of these projected vectors vary from strong detection (red) to low detection (yellow) depending on the alignment difference between the sensor detection vector (black dotted) and the wave vector (**A**).

This detection strategy was applied to a set of distributed sensors inspired by the body morphology of the leech species *Hirudo Verbana*. The leech was modeled as a 2D ellipse that is 10 cm

along its major axis and 1 cm along its minor axis. It has 24 sensors equally spaced around its perimeter at 15° increments. Each sensor has a detection vector that points away from the agent's body and is perpendicular to the tangent of the sensor's location (Fig. 3A). To detect an oncoming water wave, the wave vector at the sensor's location must be less than 90 degrees from the sensor detection vector. If this condition is met, then the wave vector is projected onto the sensor detection vector (Fig. 3B) to find the wave vector's normal component (the component of the vector pointing straight at the sensor). This computation approximates the stimulus strength at a given sensor as shown by following equation,

$$I_i = \frac{\mathbf{w} \cdot \boldsymbol{d_i}}{\|\mathbf{w}\|} \quad \text{(Eq. 2)}$$

where the dot product is taken between the water vector ($\mathbf{w}$) and the sensor detection vector at the ith sensor ($\mathbf{d_i}$). The magnitude of this projected vector and the angular displacement of the sensor from the agent's orientation (θ_i) are stored in two 1D arrays. The arrays are sent to the neural field as the components of a set of polar vectors for neural processing.

2.3 Neural Field: Winner-take-all model

At a high level, a neural field is composed of neural nodes, each of which interact with each other through excitatory and inhibitory connections (Wilson, 1999). The nodes represent populations of neurons, and each node is a pool of neurons that responds to a preferred input. In this study, the standard agent was a neural field with 24 neural nodes (matching the sensor quantity), each sensitive to specific directional inputs. The neural nodes were processed with an activation function and convolved with a synaptic weighting array to simulate neural excitation and inhibition. These functions resulted in a neural node with the highest activation (i.e., the "winning neuron"). Since each node encodes for a physical direction, as illustrated in Fig. 4 by the differently oriented arrows placed in each node, the winning neuron’s encoded direction is outputted as the perceived direction for the agent. The first step to finding this final perceived direction is processing the raw inputs from the sensors.

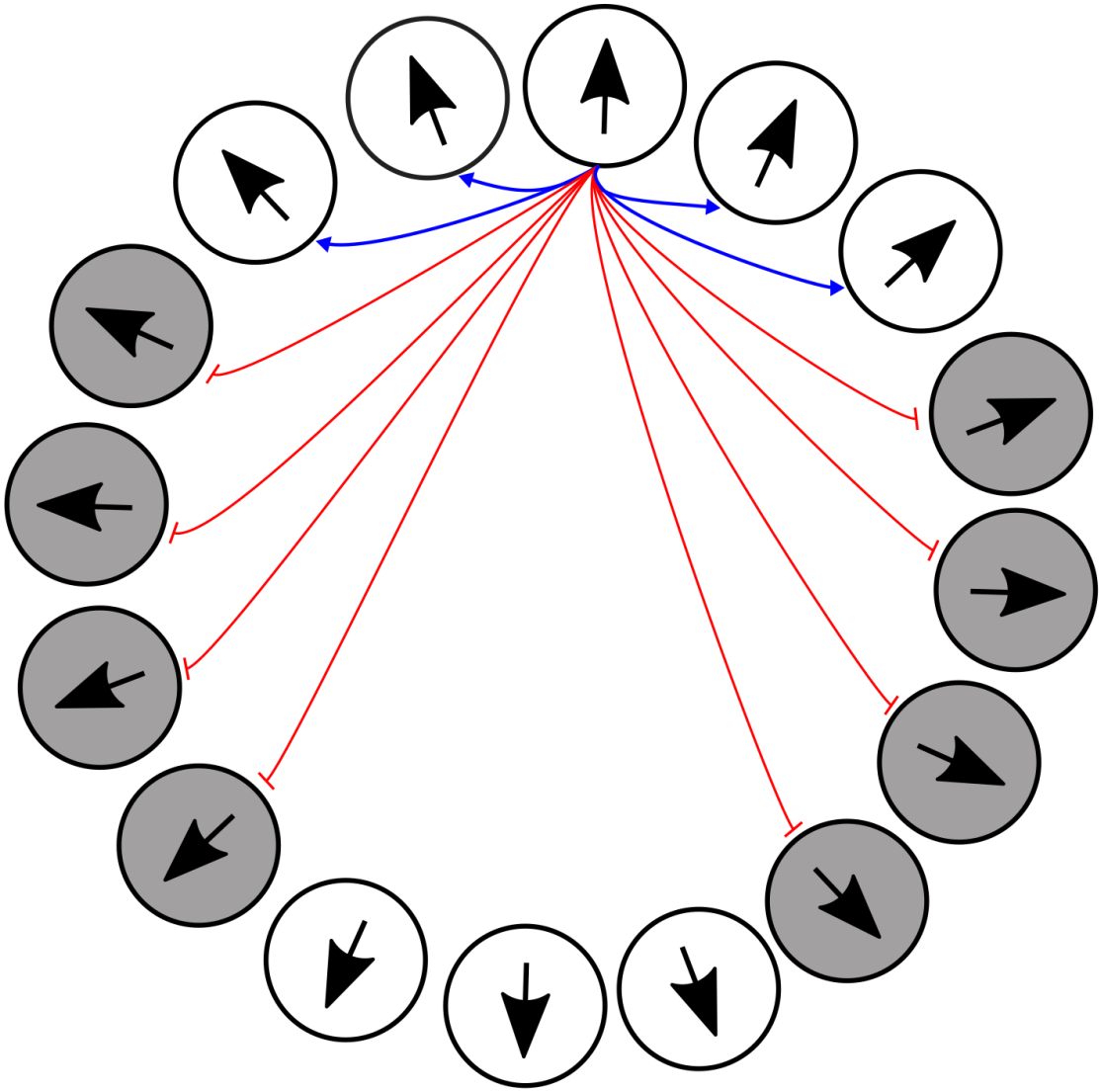

Fig. 4 Visual representation of a WTA neural field network. In this example the upper middle node receives a sensor input and sends out excitatory (blue) and inhibitory (red) signals to its surrounding nodes. Note that these excitatory and inhibitory connections occur between every single node, resulting in a fully connected network. The grayed out nodes represent nodes with a neural activation of zero, indicating that their encoded direction will not be considered for motion control.

The raw inputs sent to the neural field as two 1D arrays ($[I_1, I_2, ..., I_n]$, $[\theta_1, \theta_2, ..., \theta_n]$ as seen in Fig. 1) carry the angular and intensity information about the sensed stimulus (intensity being the magnitude of the sensed wave vector). The raw inputs undergo a cosine weighting function to determine which neural nodes should receive inputs. The processed inputs are stored in E_Ω and are calculated with the following equation,

$$E_\Omega = \sum_{i=1}^{N} I_i cos(\Omega - \theta_i) - C \quad \text{(Eq. 3a)}$$

where N is the length of the input arrays, θ is the vector holding angular inputs, I_i is the vector holding intensity inputs, and C is a constant inhibition acting on the entire neural field. Note that E_Ω refers to a single node in the network and a vectorized version of this computation operates on the entire population of nodes. E_Ω is then inserted into the differential equation that describes the behavior of the neural field,

$$\tau \frac{dR_\Omega}{dt} = -R_\Omega + (E_\Omega - W * R_\Omega)_+ \quad \text{(Eq. 3b)}$$

where R_Ω is a matrix that stores the neural response of every node at each time step and W is the synaptic weighting array responsible for encoding the inhibitory and excitatory connections between the nodes. R_Ω undergoes a convolution with W, a function commonly used in computer vision for image edge detection, but in this case was used to highlight the strongest sensory inputs while dampening weaker inputs (as seen in Fig. 5A with excitatory and inhibitory connections between the nodes). The + subscript indicates a nonlinearity function setting any neural activation value lower than zero equal to zero. This simulates how sensory neurons cease firing when no stimulus is present.

R_Ω updates every time step throughout the simulation. For most experiments, the neural field was updated in intervals, (i.e. the sensors were activated for 2 seconds and shut off for 4 seconds). When the sensors were activated, the field received non-zero inputs, increasing the neural activation of specific nodes within the field. During the inactive periods Eq. 2a received negative inputs that cause all nodes in the field to decay at a constant rate, unless a node was already at zero. During the simulation the neural field calculated a perceived direction from the winning node via parabolic interpolation (Wilson, 1999),

$$\Omega_{max} = -k\frac{R_{max+1} - R_{max-1}}{2(R_{max+1} + R_{max-1} - 2R_{max})} - \theta_{max} \quad \text{(Eq. 3c)}$$

where R_{max} was the angle encoded at the winning node, R_{max-1} and R_{max+1} were the surrounding nodes, and θ_{max} was the stored angle associated with the winning node. Ω_{max} was used as an error value in a proportional controller,

$$\delta(t) = \delta(t-1) + k_p\Omega_{max} \quad \text{(Eq. 3d)}$$

where δ is the agent's orientation at time t and k_p is the proportional control value. This controller guides the agent in the direction of the incoming stimulus, depending on the agent sensory preferences. If there is no error, then the agent does not turn (i.e., $\delta(t) = \delta(t-1)$), and the agent moves in a straight line. The higher the error, the harder the agent turns to move towards the goal.

2.4 Simulation Setup

In both the simulations that were performed, the two-dimensional behavioral arena was set to be a square with a size of 6,889 square centimeters (83 cm by 83 cm). This was meant to roughly match the size of the behavioral area used in the animal experiments, the only difference being the square shape instead of a circle to simplify collision detection for the agent (Harley et al., 2011). The agent was given 180 seconds to explore and sense within the behavioral area and had to stay within 7 cm of the target location for at least 5 seconds to count as a find. These times were shortened from the animal experiments to reduce simulation run time, but ultimately produces similar trajectory patterns.

The simulation was initialized with the defined behavioral arena and a point source gravity wave propagating outwards from a northwestern position in the arena (Fig. 5). The agent was placed at a southeastern position in the arena and performed sensor detection measurements for 2 seconds followed by a 6 second sensor deactivation period. During the sensor deactivation period, the neural field is

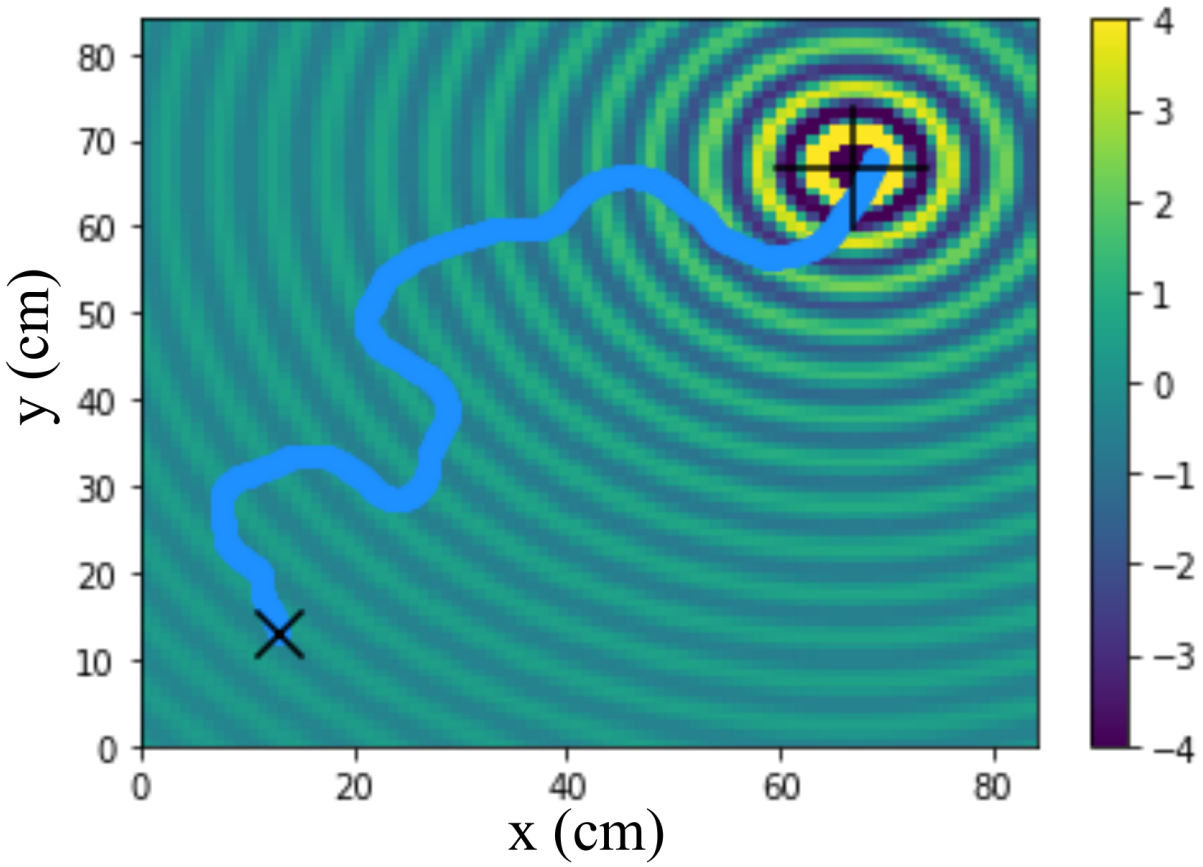

Fig. 5 Sample trajectory plot showing the path taken by an agent to reach the origin of a simulated water wave. The color bar represents the water elevation displacement (cm). Distributed sensors, like the ones shown in Fig. 3, are updated at each time step with new wave vector quantites depending on the agent's position within the arena. The simulation terminates once the agent stays inside the target location for 5 seconds. For each set of experimental parameters defined in sections 3.1 and 3.2, this navigational trial was performed 50 times.

updated with a constant decay, which acts homogeneously on all of the neural nodes. This encodes the refractory period for the neural field, allowing it to decay uniformly at a constant rate. It also gives the field a spiking pattern that is commonly observed in single celled neuron responses (Lehmkuhl et al., 2018).

At each time step, the agent used the neural field output to choose a behavioral decision. This behavioral decision was a turn rate that guides the agent around the behavioral arena. The turn rate was calculated via a proportional controller (Eq. 3d) that acts an angular error determined by the neural field. In an ideal scenario, where the agent is placed in an environment consisting of the most preferential water wave stimulus in the absence of noise, this angular error would be the angle between the agent's orientation and the direction of the stimulus, resulting in near perfect navigation. However, this is often not the case and the agent must choose the angular error by selecting it from a set of activated neural nodes (each neural node holds directional information in the form of an angle). Neural nodes are added to this set only if they surpass a neural threshold. This method determines the disorientation of the agent when performing turn behaviors. For example, in an overstimulated neural field, most of the neural nodes would surpass this neural threshold causing the agent to perform a turn that is most likely not in the direction of the incoming stimulus. In a normally stimulated neural field, one in which only the winning neuron surpasses this neural threshold, the agent would perform near perfect navigation since there is only one angular error to choose from.

Occasionally the neural field may return an empty set of activated neural nodes. This occurs either when the neural field is under stimulated or during the sensor deactivation period. In this case, the agent performs a random turn and has a 50% chance of moving forward. When the neural field returns a non empty set, the agent performs the turn and has a 75% chance of moving forward. These decisions are approximated based on a study which measured the probability of certain locomotion behaviors of leeches when given a stimulus or no stimulus (Harley and Wagenaar, 2014). During over stimulation, the agent performs virtually random movements, roughly equivalent to the swimming locomotion of the leech, which is hypothesized to be an escape behavior in response to high intensity stimuli.

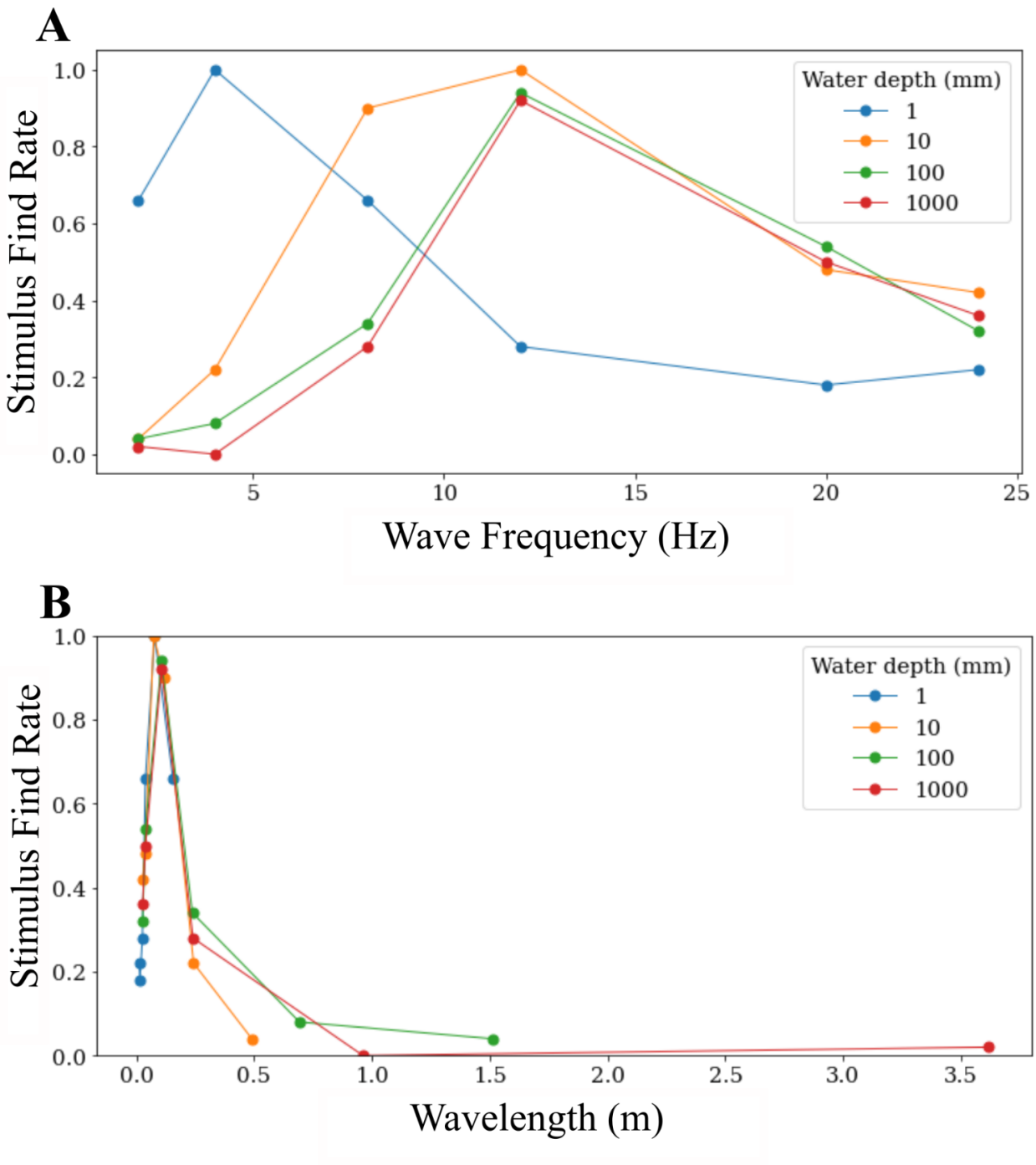

Fig 6. Find rate data for the validation simulations as a function of wave frequency and wavelength. Note that the find rates for both plots are from the same simulations plotted using different independent variables. The model preferentially responds to certain wave frequencies, similarly seen in the animal experiments (**A**). The model responds to a narrow range of wavelengths since it was encoded to detect wavenumber value and direction (**B**).

3. Results

The navigational success of the agent was measured with find rate quantities. The find rate is defined to be the proportion of successful finds over the total number of trials for a given set of parameters. Find rates approaching 1 indicate accurate navigational behavior while find rates approaching zero indicate poor navigational behavior and disorientation. When a find occurred during the simulation, the trail was terminated and marked as a successful navigation. The following data is expressed as find rate as a function of either wave frequency or wavelength. We used this method to measure navigational success so we can compare the modeled results to the past and potentially future animal results (Harley et al., 2011). Two simulations are presented below. The first simulation is meant to produce data that acts as a benchmark for validating the model's behavior and comparing the results to existing animal behavioral results. The second simulation shows the experimentation that can be done using the model.

3.1 Model Validation

Validating the model was a necessary first step before showcasing it as a method to answer questions about leech sensing and behavior. In the first round of simulations, the purpose was to calibrate the model so it could output a find rate curve due to wave frequency that matched the find rate curves found in laboratory controlled animal experiments (Harley et al., 2011). Upon validation of the model, this specific set of sensory and neural processing parameters were used as the simulation control groups.

Fig. 5 shows the navigational behavior for an agent with 24 sensors and a size of 10 cm by 1 cm, which is approximately the size of an adult medicinal leech. Tests were performed at four different simulated water depths to ensure the neural field was calibrated correctly. The original animal experiments were performed at 20 mm and outputted a response curve that matched the response curve in Fig. 5A at a simulated water depth of 10 mm (orange).

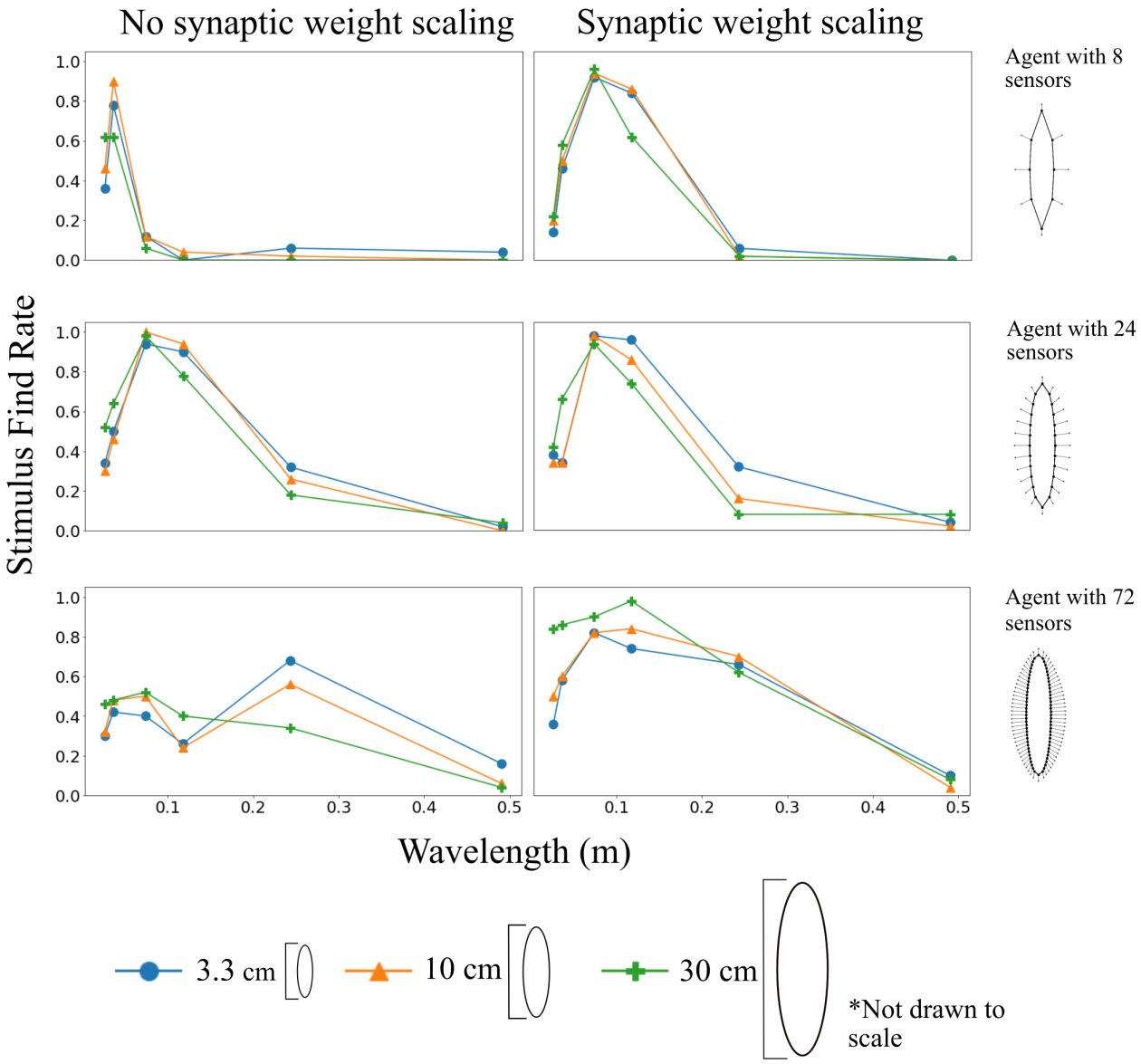

Fig. 6 Find rate data for two different neural field configurations. The left column shows find rate data when the synaptic weighting array was not scaled according to the quantity of neural nodes in the network. The right column shows find rate data when the neural node quantity was scaled according to the sensor quantity. The data in each row corresponds to a specific sensor quanity (8, 24, 72) and each color corresponds to the agent's height (3.3 cm, 10 cm, 30 cm). A total of 18 experimental trials were performed (3 sizes x 3 quantities x 2 configurations = 18) with the control being the agent with 24 sensors and a height of 10 cm.

Fig. 5B shows that the find rate depends on a narrow range of wavelengths. This occurred because the sensors detect the wavenumber, which is the inverse of wavelength, resulting in the neural field responding only to certain wavelength values. It is only known how leeches respond due to frequency so we can only hypothesize how leeches respond to wavelength, but the formulation of this model ensures that it's behavior matches the frequency preferences of an adult leech at the specified water depth. This data functions as a validation to confirm that the agent behaved correctly with the chosen set of parameters.

3.2 Neural Field Experiments

Assuming that the standard agent (of size 10 cm by 1 cm with 24 neural nodes and 24 sensors) matches the average adult leech morphology of the species *Hirudo Verbana* from Harley's 2011 study, further experiments were done to measure the changes in navigational behavior as the size, sensor quantity, and synaptic weighting array were altered (as shown in Fig. 6 with the various sensor layouts and agent sizes). The following experiment measures find rate as a function of wavelength for 9 different agent compositions: 3 different sizes and 3 different sensor quantities. The size of the agent and the sensory quantity was scaled up and down by a factor of three resulting in agent sizes with the dimensions of 0.3 cm by 3.3 cm, 1 cm by 10 cm, and 3 cm by 30 cm, and agent sensor quantities of 8, 24, and 72. All trials were performed at a water depth of 10 mm.

This experiment was performed twice: once where the length of the synaptic weighting array was kept constant, and once where the length of the synaptic weighting array was changed based on the neural node quantity (same as sensor quantity). The synaptic weighting array can be visualized in Fig. 4 as an array defining the excitatory and inhibitory connections between the neural nodes. Essentially, this synaptic weight scaling simulates the changes within the nervous system as the leech develops and becomes more complex. This experiment tests a variety of parameters that define the agent's sensory capabilities. The data was split up into 6 plots: one column of 3 plots showing find rate data when the synaptic weighting array was kept constant and another column of 3 plots showing find rate data with the scaled synaptic weighting array.

Fig. 6 suggests that sensor quantity directly impacts the agent's wavelength preference as shown by the variation of find rate curves from row to row. The data also implies that an agent with more sensors will have increased navigational success in response to larger wavelengths. In the absence of synaptic weight scaling (left column), the range of sensory preference increased as the sensor quantity increased. This similar trend occurred when there was synaptic weight scaling, but to a smaller degree as the find rate curves for 8 sensors and 24 sensors were generally the same. It is also interesting to note that the find rate curves remained almost the same across all agent sizes which was an unexpected result.

4. Discussion

The results indicate that the model can successfully replicate leech navigation in response to mechanical water wave stimuli and can match the mechanosensory preferences of adult leeches. The find rate curve in Fig. 5A at a depth of 10 mm closely matches the find rate curve from the literature (Harley et al., 2011), demonstrating that dynamic neural fields can be properly tuned to process sensory information. Note that this model is purely theoretical and has not been optimized but still managed to deliver accurate results.

Furthermore, the additional experiments display how easily the model parameters can be varied to test questions about stimulus detection, sensor layout, neural field sensory processing, agent size, and more. Fig. 6 shows that increasing sensor quantity with a scaled synaptic weighting array increases the range of preferable wavelengths but decreasing sensor quantity with a scaled synaptic weighting array results in find rates that almost exactly match the original sensory preferences. These results suggest that the model successfully incorporates a form of graceful degradation (sensory processing that does not fail as sensor quantity decreases) and performance improvements as the number of sensors increase. Also, varying sensor quantity and agent size can be a valuable tool to study the changes in behavior due to different animal morphologies (change in sensor layouts). It would normally take excess time and money to perform laboratory experiments on multiple species of leech to answer this question but conducting the experiments in simulation could provide valuable preliminary results and potential conclusions.

The model presented in this study acts as a framework for future studies that aim to answer questions about how animal nervous systems transform sensory information into behavioral outputs. It offers a fast and low-cost way to test the impact of different sensory detection mechanisms on navigational behavior. Current studies are using this model to answer questions about the leech's preference to either wave frequency or wavelength. The goal is to test various mechanical sensing techniques, such pressure sensing, horizontal velocity sensing, and mechanotransduction via distributed cilia, to measure navigational success at a range of water depths and water wave conditions. Other studies aim to measure the effectiveness of using dynamic neural fields for the sensory processing of magnetic field stimuli. This study will be done both in simulation and with hardware to predict how information from magnetoreceptors might be processed by the nervous system.

The presented simulation study displays how specific computational techniques can be combined and adapted to learn about and replicate animal sensory systems and behavior. It offers a complete model that can be easily expanded with high fidelity components based on the biology and behavior of animals. It will also lead towards more complex navigational hardware systems that require novel sensory processing techniques. Future studies are currently in the works to improve this model and use it for more bioinspired and biomimetic purposes.

Acknowledgments

I would first like to thank UNC's Office of Undergraduate Research and Summer Academic Programs for funding one of my research courses during the 2020 summer, which helped kickstart this project. I would like to thank Dr. Catherine Kehl and Dr. Cynthia Harley for all their expert guidance throughout this project. I want to directly thank Dr. Brian Taylor for his generous mentorship and kindness. I would like to acknowledge the rest of the members of the QBES Lab for their support, as well as Dr. Amy Maddox and all my peers who completed an Honors Thesis in biology for their thoughtful feedback.

References

1. Amari, S. (1977) “Dynamics of pattern formation in lateral-inhibition type neural fields.” Biol. Cybern. 27, 77–87
2. Bezares-Calderón, L.A., Berger, J., Jékely, G. (2019) “Diversity of cilia-based mechanosensory systems and their functions in marine animal behaviour.” Phil. Trans. R. Soc. B 375: 20190376
3. Coombes, S., et al. (2014) “Neural Fields: Theory and Applications.” Berlin Heidelberg, Springer-Verlag
4. Govedich, F.R. and Bain, B.A. (2005) “All about the leeches of montezuma wall.” https://www.nps.gov/moca/learn/nature/upload/montezuma_well_leeches.pdf
5. Harley C.M., Asplen M.K. (2018) “Annelid Vision.” Oxford Research Encyclopedias
6. Harley C.M., Cienfuegos J., Wagenaar D.A. (2011) “Developmentally regulated multisensory integration for prey localization in the medicinal leech.” J Theor Biol 214: 3801-3807
7. Harley C.M., Wagenaar D.A. (2014) “Scanning Behavior in the Medicinal Leech Hirudo verbana.” PLoS ONE 9(1): e86120
8. Hochner, B. (2012) “An Embodied View of Octopus Neurobiology.” Current Biology 22 (20): R887–92
9. Hunt, A., et al. (2017) "Development and Training of a Neural Controller for Hind Leg Walking in a Dog Robot." Frontiers in Neurorobotics 11(18)
10. Izhikevich, E.M. (2010) “Dynamical Systems in Neuroscience.” MIT Press
11. Jensen, K.K. (2010) “Light-dependent orientation responses in animals can be explained by a model of compass cue integration.” J Theor Biol 262: 129-141
12. Kasabov, N.K. (2019) “Time-Space, Spiking Neural Networks and Brain-Inspired Artificial Intelligence.” Berlin, Springer-Verlag
13. Kristan W.B., Calabrese R.L., & Friesen W.O. (2005) “Neural control of leech behavior.” Progress in Neurobiology. 76: 279-327

14. Lehmkuhl A.M., Muthusamy A., & Wagenaar D.A. (2018) “Responses to mechanically and visually cued water waves in the nervous system of the medicinal leech.” J Exp Biol 221(4): jeb171728
15. Lockery S.R., & Kristan W.B. (1990) “Distributed processing of sensory information in the leech. I. Input- output relations of the local bending reflex.” J Neurosci 10 (6): 1811-1815
16. McDonnell, M.D., et al. (2014). "Engineering intelligent electronic systems based on computational neuroscience." Proceedings of the IEEE 102(5): 646-651
17. Moshtagh-Khorasani, M., Miller E.W., & Torre, V. (2013) “The spontaneous electrical activity of neurons in leech ganglia.” Physiol Rep 1: e00089
18. Nichols, S.T., Kehl, C.E., Taylor B.K., Harley, C. (2020) “Bioinspired navigation based on distributed sensing in the leech.” Living Machines 2020, LNAI 12413, pp. 275–287
19. Taylor, B.K. (2016) “Validating a model for detecting magnetic field intensity using dynamic neural fields.” J Theor Biol 408: 53-65
20. Taylor, B.K. (2017) “Bioinspired magnetic reception and multimodal sensing.” Biol Cybern 111: 287-308
21. Wagenaar, D.A. (2015) “A classic model animal in the 21st century: recent lessons from the leech nervous system.” J Exp Biol 218: 3353-3359
22. Wilson, H. (1999) “Spikes, Decisions, and Actions: The dynamical foundations of neuroscience. New York.” Oxford University Press
23. Zhang, K. (1996) “Representation of spatial orientation by the intrinsic dynamics of the head-direction cell ensemble: a theory.” The Journal of Neuroscience 16(6): 2112-2126
24. Zimmerman, A., Bai, L., & Ginty, D.D. (2014) “The gentle touch receptors of mammalian skin.” Science 346(6212), 950–954